

# Investigating molecular mechanism for the stability of ternary systems containing cetrimide, fatty alcohol and water by using computer simulation

Vu Dang Hoang,<sup>1</sup> Hung Huu Tran,<sup>2</sup> Cao Cong Phuong,<sup>3</sup> Hue Minh Thi Nguyen,<sup>2</sup> and Toan T. Nguyen<sup>3, \*</sup>

<sup>1</sup>*Department of Analytical Chemistry and Toxicology,  
Hanoi University of Pharmacy, 13-15 Le Thanh Tong, Hoan Kiem, Hanoi, Vietnam*

<sup>2</sup>*Faculty of Chemistry and Center for Computational Science,*

*Hanoi National University of Education, 136 Xuan Thuy Street, Cau Giay, Hanoi, Vietnam*

<sup>3</sup>*Faculty of Physics and VNU Key Laboratory on Multiscale Simulation of Complex Systems,  
VNU University of Science, Vietnam National University,  
334 Nguyen Trai Street, Thanh Xuan, Hanoi, Vietnam*

Computer simulations using atomistic model are carried out to investigate the stability of ternary systems of pure or mixed fatty alcohols, cetrimide, and water. These semi-solid oil-in-water systems are used as the main component of pharmaceutical creams. Experiments show that the mixed alcohol systems are more stable than pure ones. The current experimental hypothesis is that this is the result of the length mismatch of the alkyl chains. This leads to higher configurational entropy of the chain tip of the longer alcohol molecules. Our simulation results support this hypothesis. The results also show that the shorter alcohol molecules become stiffer with higher values of the deuterium order parameters and smaller area per molecule. The magnitude in fluctuations in the area per molecule also increases in mixed systems, indicating a higher configurational entropy. Analysis of the molecular structure of simulated systems also shows good agreements with experimental data.

PACS numbers: 87.16.D, 88.20.fj, 87.10.Tf, 81.16.Dn, 87.16.A-, 82.70.Uv

## I. INTRODUCTION

Pharmaceutical creams are one of the common types of topical formulations, used as a means of delivering an active ingredient directly to the skin. Generally speaking, they are oil-in-water semisolid emulsions.

According to the gel network theory [1, 2], these formulations consist of at least four phases: (i) crystalline/hydrophilic gel phase is composed of bilayers of surfactant and fatty amphiphile and water molecules are inserted between the bilayers (i.e. interlamellarly fixed water); (ii) water molecules bound as free bulk water are in equilibrium with the interlamellarly fixed water in the gel phase; (iii) lipophilic gel phase is built up by the excess of the fatty amphiphile, which is not part of the hydrophilic gel phase; and (iv) dispersed oil phase (i.e. inner phase) is mainly immobilized mechanically from the lipophilic gel phase. In practice, surfactant-fatty alcohol-water ternary systems could be used as representative models of the continuous phases of the corresponding semisolid o/w emulsions. Previous works on the characterization of semisolid oil-in-water emulsions containing pure and mixed homologue fatty alcohols (i.e. cetyl, stearyl and cetostearyl alcohols) and cetrimide [3–5] have shown that the oil-in-water emulsions increased in consistency and remained stable on the addition of cetostearyl alcohol, whereas the emulsion stability decreased markedly to mobile liquid when cetyl or stearyl alcohol was added individually on the preparation. This is demonstrated in the phase diagram, Fig. 1, where it

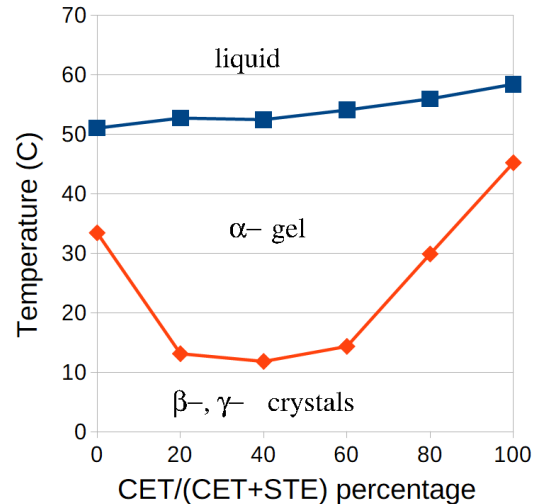


FIG. 1: (Color online) The phase diagram of the mixture of stearyl and cetyl alcohol at various temperature and mixing ratio. The  $\alpha$ -gel (liquid crystal) exists to relatively low temperature while for pure cetyl or stearyl bilayers, the  $L_\beta$  crystal phase exists at higher temperature [3].

is shown that the  $\alpha$ -gel is stable down to lower temperature for mixed cetyl and stearyl alcohol as compared to either of them individually.

Although the above-mentioned studies partially showed the correlation between various fatty alcohol combinations and their influence on the microstructure and consistency of the corresponding oil-in-water emulsions prepared with them, no comprehensive studies at

\* Corresponding author: toannt@hus.edu.vn

the molecular level has been carried out. The aim of this study is to elucidate the molecular mechanism for the higher stability of the mixed cetostearyl bilayer  $\alpha$ -gel network as compared to each component used separately. Previous experiments [3, 6] suggested this is due to the alkyl chain length mismatch in the mixed system. As a result, the alkyl chain tip of C18OH has a high degree of freedom, and, in this part *gauche* coordination increases. Our computational study supports this hypothesis at the molecular level. We also show that upon mixing the alkyl chain of C16OH becomes stiffer and the C18OH alkyl chain tip becomes more flexible. Also, the in-plane area per molecule fluctuations is more pronounced for mixed systems. This explanation provides further insights into the molecular mechanism of the stability of mixed system.

The paper is organized as follows. After the Introduction section, in Sec. II, the model of our system and various physical parameters used in the simulation are presented in details. In Sec. III, the results are presented and their relevance to available experimental data is discussed. We conclude in Sec. IV.

## II. COMPUTATIONAL DETAILS

The chemical structure of cetyl ( $\text{CH}_3(\text{CH}_2)_{15}\text{OH}$ ), stearyl ( $\text{CH}_3(\text{CH}_2)_{17}\text{OH}$ ) alcohols and cetrimide ( $\text{C}_{17}\text{H}_{38}\text{BrN}$ ) are downloaded from pubchem database (<https://pubchem.ncbi.nlm.nih.gov/>) with CID 2682, 8221 and 14250 respectively. Gaussian 09 software package is used to optimize their three dimensional structures, and to calculate the partial charges on each atom. These partial charges are then adjusted and rounded to match the values of the hydrocarbon tails, hydroxyl and choline head groups of forcefield for the united atom model for polyalcohols [7] and of the lipid forcefields [8, 9]. These parameters are then combined with the bonded interactions in the Amber GAFF forcefield by using AmberTools 2017 to create the full forcefield for the molecules used in the computer simulations. For the bromide ions, the AMBER99-ILDN forcefield is used. For the water molecules, the common TIP3P forcefield is used for its high compatibility with the AMBER forcefields.

The initial coordinates of the atoms of a bilayer of these molecules are then constructed in the following way. First, the corresponding optimized atom coordinates in the previous step are duplicated at random site in either a square or hexagonal lattice in the  $xy$ -plane with a lattice constant of 0.48nm. The hydrocarbon tails are directed inward the bilayer along the  $z$ -axis, while the hydroxyl polar group are exposed outward the solution (see Fig. 2). We prepare the system of cetyl and stearyl alcohol mixture at 100:0, 70:30, 50:50, 30:70, 0:100 number ratios. For easy identification in later discussion, we name these systems 100CET, 70CET, 50CET, 30CET, and 0CET respectively. Beside the alcohol molecules,

System name	0CET	30CET	50CET	70CET	100CET
STE:CET # ratio	100:0	70:30	50:50	30:70	0:100
# of Cetyl	0	176	292	408	584
# of Stearyl	584	408	292	176	0
# of Cetrimide	64	64	64	64	64
# of Br ions	64	64	64	64	64
# of water molecules	37146	37146	37146	37146	37146

TABLE I: The five systems simulated in this work with different number ratios of stearyl:cetyl alcohol molecules varying from 0 to 100%. The name of the system listed will be used throughout this paper for easy identification. The last five rows list the number of molecules for different species of molecules of the simulated systems.

there are also positively charged cetrimide molecules embedded in the bilayer to make them stable. Their number is about 10% of the total number to match experimental systems. The bilayer is then solvated with 37210 water molecules, creating simulation box of about 24nm along the  $z$ -axis. The electrostatic repulsion between parallel bilayer among these cetrimide molecules keeps the bilayer structure stable. To compensate for the charges of cetrimide, the system is made neutral by replacing randomly 64 water molecules by bromide ions,  $\text{Br}^-$ .

The periodic boundary condition is used for all three directions. The thickness of the water layer (24 nm) has been chosen so that it is much larger than the typical electrostatic screening in the system (about 1nm) and the electrostatic coupling between neighboring simulation boxes is well screened out. This value also lies in the range of the repeat distance of these cetyl/stearyl lamellar value from 6 to 100nm [10] while keeping the computational cost reasonable. For reference, the number of each type of molecules for each of our simulated systems are listed in Table. I. Particle Mesh Ewald method [11] was used to treat the long-range electrostatic interaction with a real space cutoff of 1.4 nm. Van der Waals interactions are also cut off at 1.4 nm, with the appropriate cut-off corrections added to pressure and energy.

After constructing the initial coordinates of the atoms and topology of the molecules, the systems are further processed and simulated by using GROMACS 2018.3 molecular dynamics software package [12, 13]. The whole system of surfactants, water and ions are equilibrated for 100 ns at temperature 300K and pressure of 1 atm by using NPT ensemble using Berendsen thermostat and barostat. The barostat maintains independently the pressure along each of the three directions  $x$ ,  $y$  and  $z$  axes of the system. This ensures that each dimension of the simulation box varies independently from each other, allowing the bilayer molecules to relax into its optimal lattice structure regardless of the initial lattice configuration.

For production run, the systems are simulated for additional  $1\mu s$  at the same temperature and pressure by using Nose–Hoover thermostat and Parrinello–Rahman barostat. All barostats are kept at 1 atm so that on average the surface tension of the bilayers simulated are zero. For taking statistics, all the configurations within the first 100ns of simulation, where the systems are relaxing to its equilibrium state, are dropped. All the simulations are performed on the High Performance Computing cluster of the VNU Key Laboratory for Multiscale simulation of complex systems at the Vietnam National University – Hanoi. For analysis, beside standard tools from GROMACS software, the VMD software package [14] and MEMBPLUGIN plugin [15] is used for visualization, calculation of the order parameters, area per molecules, tilt angles, and other physical properties of the bilayer.

### III. RESULTS AND DISCUSSIONS

Experimentally, it is established by various synchrotron X–ray studies that the lamellar bilayer of the cetyl, stearyl alcohols is of hexagonal lattice packing with diffraction spacing of  $4.06\text{\AA}$  for the amount of water and temperature that we simulate [3, 10, 16, 17]. This corresponds to the hexagonal lattice with lattice constant (or nearest neighbor distance) of  $4.06\text{\AA} \times 2/\sqrt{3} = 4.69\text{\AA}$  and the area per molecule of  $19.13\text{\AA}^2$ . Additionally, in experimental studies of on the bilayer made of different types of molecules with different chain lengths and head groups, it is shown that this in–plane lattice distance depends very weakly on the length of the hydrocarbon chain, and mostly depends on the interaction among the head groups [18]. Therefore, our immediate concerns are to reproduce these experimental facts to verify that our forcefield parameters are reasonable.

#### A. Relaxation to equilibrium

The first question one would like to address is whether our systems have sufficient time within our simulation to relax into its equilibrium structure, at least at short range order. To do this, two very different initial starting configurations of the bilayer is used (see Fig. 2). In the first starting configuration, the 292 alcohol molecules and 32 cetrimide molecules in each leaflet are positioned randomly at the sites of a  $18 \times 18$  square lattice with a lattice constant of  $0.48\text{nm}$  (Fig. 2a). The initial simulation box dimension in the in–plane direction is  $8.46\text{nm} \times 8.46\text{nm}$ . In the second starting configuration, these 324 molecules are positioned at the sites of a  $18 \times 18$  hexagonal lattice with a lattice constant of  $0.46\text{nm}$  (Fig. 2b). The initial simulation box dimension in the in–plane direction is  $8.42\text{nm} \times 7.17\text{nm}$ . These two initial systems are both solvated with the same numbers of water molecules and  $\text{Br}^-$  ions as listed in Tab. I. They are then relaxed in NPT

ensemble of 1 atm and  $300^\circ\text{K}$  by using Berendsen thermostat and barostat. Each dimension of the simulation box can relax independently of each other, hence the bilayer can adopt to any optimal gel or crystal packing that minimizes the system free energy. In Fig. 2d, e and f, we plot as a function of time, the potential energy of the system per atom, the in–plane projected area per molecule, and the repeat distance of the lamellar bilayer (the  $L_z$  dimension of the box). For comparison, these quantities are also plotted for an equilibrium MD run after the systems has been equilibrated, using Nose–Hoover thermostat and Parrinello–Rahman barostat. As one can clearly sees, after at most 20ns, all our quantities converge to their equilibrium value regardless of initial starting configuration. The convergence is rather remarkable based on the fact that the individual  $xy$  dimensions of the box,  $L_x$  and  $L_y$ , remain very different for different starting configurations, but the in–plane area per molecule

$$\sigma = L_x \times L_y / 324,$$

is the same for all simulations within statistical errors. Although, these graph are plotted for the 0CET system, data for all other four systems (not plotted) show similar behaviours. All the relevant parameters of the system converged after about 20ns of relaxation. Additionally, as we will see in the next section, the local order for the alcohol molecules in the bilayer is indeed hexagonal packing with lattice spacing of  $4.69\text{\AA}$  in excellent agreement with high angle X–ray diffraction data.

In light of these results, for the rest of this paper, unless explicitly stated, all systems are initialized very closed to their equilibrium structure by using hexagonal lattice starting configuration to minimize the relaxation time of each system. Furthermore, in each analysis for equilibrium properties, data from the first 100ns of a MD production run is dropped to make sure the systems are well equilibrated.

#### B. Molecular structure of the bilayers

Let us turn now to describe the molecular structure of the bilayer to show that they reproduce well the available experimental data as well as provide additional insights obtained from the simulations. First, the in–plane radial distribution function,  $g(r)$ , of the carbon atoms in the hydrocarbon tail of the molecules are calculated. This is the probability of an atom being at the radial distance from a given atom. Only the in–plane  $xy$  components of the atom positions are used for this calculation. In Fig. 3a, the radial distribution for the tenth carbon atom (counted from the OH polar head) deep in the leaflets are plotted for the systems with 100% cetyl alcohol and 100% stearyl alcohol. As one can sees, the first two peaks of these distribution functions occur at almost the same locations regardless of the length of the hydrocarbon chain. This also means that the nearest neighbor distance between the alcohols is nearly independent of the length

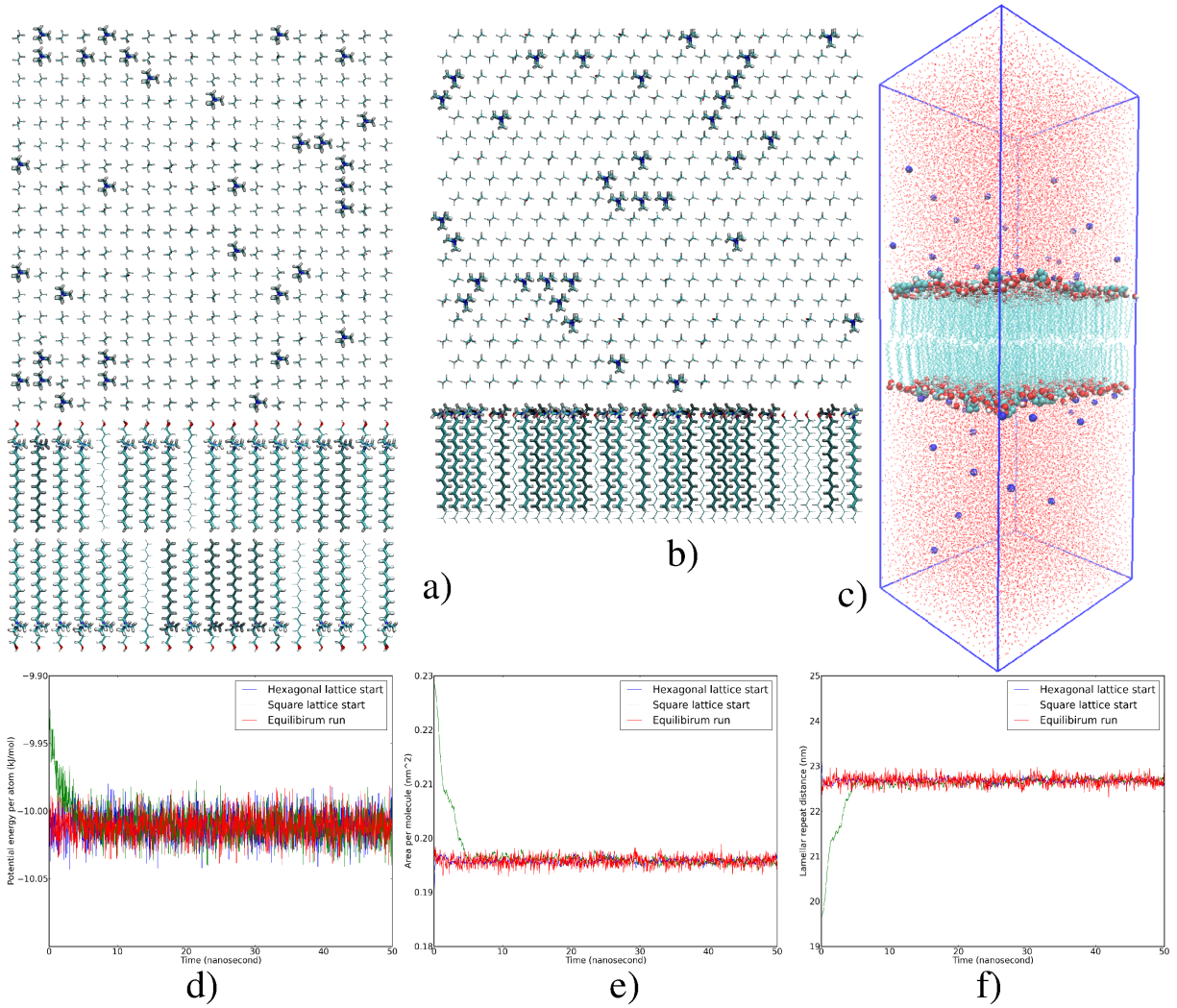


FIG. 2: (Color online) (a) Top view and side view of the square lattice starting configuration of the bilayer of alcohol molecules. The hydrocarbon tails of the molecules are aligned along the  $z$  axis with the polar groups exposed to the outside of the bilayer. In the  $xy$  plane, they are arranged into a square lattice of lattice constant  $0.48\text{nm}$ . The cetrimide molecules are drawn using thicker lines for clarity. (b) Top and side views of the hexagonal lattice starting configuration of the bilayer. (c) A typical snapshot of our simulation system during simulation showing the bilayer membrane fluctuates in explicit water molecules (pink) and neutralizing bromide ions (blue). The periodic simulation box is shown using by blue lines. (d) The relaxation of the potential energy for different starting configurations. The same quantities obtained from a well-equilibrated system is plotted for comparison. (e) and (f) similar to (d) but the quantities plotted are the in-plane projected area per molecule and the lamellar repeat distance.

of the hydrocarbon chains for the two lengths simulated. This suggests that the hydrocarbon tail plays small roles in determining the projected area per molecules of these bilayers. Rather, it would be the head group (both are OH group for our molecules) that determine the position of the peaks, as supported by experimental studies [18].

Although, depending on the specific lipids, the lamella phases can be orthorhombic, monoclinic or hexagonal crystals, the cetyl and stearyl mixture is known to exhibit hexagonal order in lamella phases:  $\alpha$ -gel at higher temperature, and  $L_\beta$  crystals at lower temperature. X-ray

experiments [10] shows hexagonal order with the diffraction spacing of  $4.06\text{\AA}$  for various cetostearyl alcohol ternary gel. This translates into the nearest neighbor distance of  $4.69\text{\AA}$  and an unit cell area of  $19.13\text{\AA}^2$ . Our simulation agrees well with these experimental facts. Even though the starting configuration is that of either a square lattice or hexagonal lattice of lattice constant  $4.8\text{\AA}$ , both systems settle to an equilibrium hexagonal order. Figure 3a shows that the most probable nearest neighbor distance of our alcohol molecules projected on the  $xy$  plane is  $a = 4.69\text{\AA}$  in excellent match to ex-

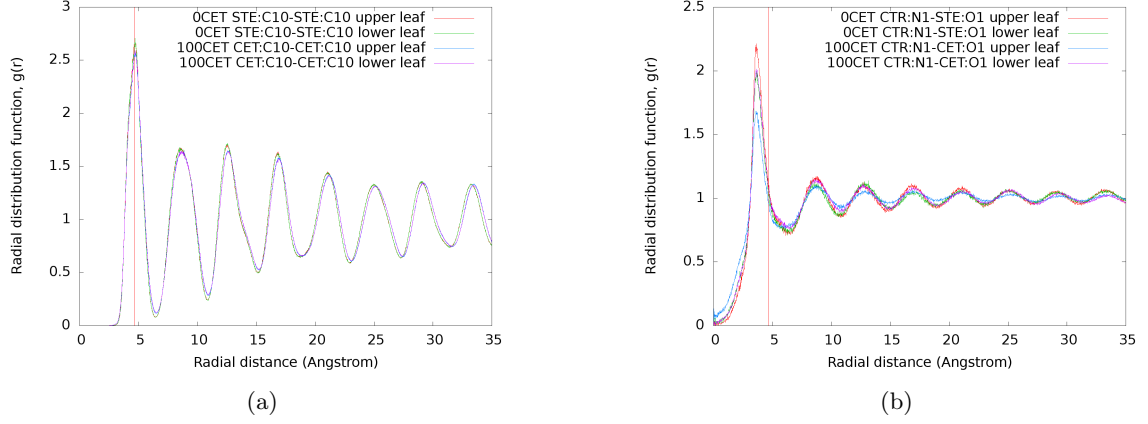


FIG. 3: (Color online) (a) The in-plane  $xy$  radial distribution of the alcohol molecules calculated based on the position of the 10th carbon atom (counting from the  $-OH$  head group) of the bilayers of 0CET and 100CET systems. In each system, the upper and lower leaflets of the bilayer are calculated separately. (b) The in-plane  $xy$  radial distribution function of the oxygen atom of the polar ( $-OH$ ) head group of the alcohol molecules around the nitrogen atom of the positively charged ( $N(CH_3)_3$ ) head group of the cetrimide. The red vertical line is at  $r = 4.69\text{\AA}$  in both a) and b) subfigures.

System	$L_x(\text{nm})$	$L_y(\text{nm})$	$L_z(\text{nm})$	$\sigma(\text{nm}^2)$
0CET	$8.50 \pm 0.06$	$7.38 \pm 0.05$	$23.38 \pm 0.09$	$0.194 \pm 0.003$
30CET	$8.51 \pm 0.05$	$7.40 \pm 0.04$	$23.17 \pm 0.09$	$0.194 \pm 0.003$
50CET	$8.54 \pm 0.05$	$7.39 \pm 0.04$	$23.02 \pm 0.09$	$0.195 \pm 0.003$
70CET	$8.54 \pm 0.05$	$7.41 \pm 0.04$	$22.88 \pm 0.09$	$0.195 \pm 0.003$
100CET	$8.56 \pm 0.05$	$7.41 \pm 0.04$	$22.68 \pm 0.09$	$0.196 \pm 0.003$

TABLE II: The average dimensions of the simulation box and the area per molecule of the bilayers obtained from simulation.

perimental data. Furthermore, both cetyl and stearyl molecules show almost the same inter-atom distance. This suggests that the length of the alkyl chain has only a small influence on the short range order in the bilayer. The difference only shows up in a slight difference in the locations of higher order peaks in the radial distribution. This also agrees with experimental data [18] showing this length depends mostly on the type of the head group, not on the length of the alkyl chain. This provides strong support for the chosen physical parameters of the atoms and molecules that we use. Further detail investigation of these parameters will be published in a near future work, where the phase diagram and energetics of these alcohol systems are computed computationally.

One can also look at the local ordering in each leaf of the bilayer from a different perspective. In Fig. 4a, the configuration of the molecules forming the “upper” leaf of the bilayer for the system of 100% stearyl alcohol after  $1\text{ }\mu\text{s}$  of simulation is visualized by using the VMD program. A colored picture of the snapshot is taken, and then Fourier analysis is performed by using ImageJ

photo analysis program. The result is shown on Fig. 4b, where the first few order peaks of a six-fold symmetry is clearly seen. This confirms once again the hexagonal nearest neighbor peak in the radial distribution function. The  $\alpha$ -gel and  $L_\beta$  crystal lamellar phases of the alcohol bilayers are also distinguished from other phases by the fact that the hydrocarbon tail of the molecules lies parallel to the normal direction to the bilayer. This is indeed the case for our systems. In Fig. 4, the histogram of the tilt angle of the vector from C2 to C17 carbon atoms of the cetyl alcohol molecules are plotted. As one can clearly see, the hydrocarbon tail typically tilts about  $4^\circ$  from the  $z$ -axis. This small angle shows that our bilayer leaflets are in lamellar  $L_\alpha$  and  $L_\beta$  phases.

Further information on the system can be obtained by investigating the electrostatic interaction in the bilayer and mobile  $\text{Br}^-$  counterions. First, one also wants to study the distribution of the neutral alcohol molecules around a charged cetrimide molecules. To this end, the radial distribution function of the head group of the alcohol molecules (represented by the position of the oxygen atom) around the head group of the cetrimide molecules (represented by the position of the nitrogen atom) in the in-plane projection is calculated. The results for different cases are shown in Fig. 3b. The lines correspond to radial distribution function in the upper and lower leaves of the bilayer for the system with 100% stearyl alcohol (red and green), and for the system with 100% cetyl alcohol (blue and violet).

From the comparison with alkyl-alkyl radial distribution function, one can clearly see from these graphs that the charged head group of the cetrimide molecules attracts the polar head group of the alcohol towards it. The first peak location is smaller than that of the alkyl first peak. The probability of finding the OH head group



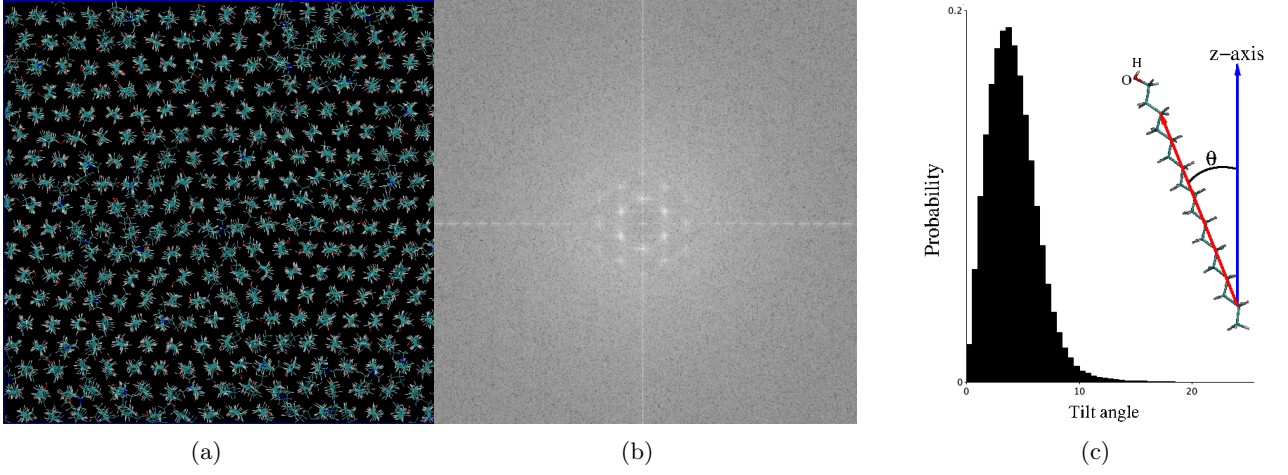


FIG. 4: (Color online) (a) Top view of the upper leaf of the bilayer for the 100% stearyl system as looking down along the  $z$  axis. Each atom appears as projection onto the  $xy$  plane. The cetrimide molecules are drawn using thicker lines for distinction. The configuration chosen is at  $1\mu s$  of the simulation. (b) Fourier transform of image in (a) showing the first few orders of a sixth-fold symmetry. (c) Histogram of the tilt angle of the alkyl to the normal direction of the bilayer, together with the graphical definition of this tilt angle.

of the alcohol near the cetrimide  $N^+(CH_3)_3$  head group is also finite at small  $r$ .

Next, one looks at the distribution of the  $Br^-$  counterions in the water layer between the bilayers. Within standard self-consistent mean-field Poisson-Boltzmann (PB) theory of electrolytes [19], the distribution of the counterions in the water solution between two infinite similarly-charged parallel planar surfaces at distance  $L_w$  is given by [20–22]:

$$\rho(z) = \frac{1/(2\pi l_B \Lambda^2)}{\cos^2[(z - L_w/2)/\Lambda]}, \quad (1)$$

where  $z$  is the normal distance from one of the surfaces;  $\sigma_e$  is the charge density per unit area of the parallel charged surface.  $l_B = e^2/4\pi\epsilon_0\epsilon_w k_B T$  is the so-called Bjerrum length of the solution,  $\epsilon_0$  is the dielectric permeability of free space, and  $\epsilon_w$  is the dielectric constant of the solution. It is the length at which two elementary charges interact with Coulomb potential energy equal to the thermal energy,  $k_B T$ . In Eq. (1),  $\Lambda$  is a length related to the thickness of the water layer  $L_w$  by the transcendental equation:

$$2\pi l_B (\sigma_e/e) \Lambda = \tan[L_w/2\Lambda]. \quad (2)$$

In application to our bilayer system,  $Br^-$  ions play the role of mobile counterions while each leaf of the bilayer plays the role of the charged planar surface with charge density

$$\sigma_e = 64e/L_x L_y$$

. For convenience, we measure the  $z$  distance from the center of the bilayer, then the PB solution can be rewritten as:

$$\rho(z) = \frac{1/(2\pi l_B \Lambda^2)}{\cos^2[(z - L_z/2)/\Lambda]}, \quad (3)$$

System	$\Lambda$ (nm)	$\epsilon_w$	$L_w$ (nm)	$V_w$ (nm <sup>3</sup> )	$d$ (nm)
0CET	6.038	76.85	18.51	1159.9	4.88
30CET	6.019	75.10	18.44	1160.1	4.74
50CET	6.015	74.59	18.42	1162.4	4.60
70CET	5.896	73.99	18.32	1158.7	4.56
100CET	5.880	74.02	18.30	1160.6	4.38

TABLE III: Fitting parameters of PB solution, Eq. (3) to the  $Br^-$  ion profile in the water layer from 3nm to the center of the water layer. See text for discussion.

Since the water solution is explicitly simulated in our system, by fitting the PB solution to the  $Br^-$  counterion profile, one can obtain the effective dielectric constant of the system as well as the water layer thickness,  $L_w$  and compare it to the above analysis. It should be noted that, due to a mismatch of the dielectric constants of the bilayer and water layer, the dielectric constant varies near the bilayer surface [23]. Taking into consideration the fact that the bilayer is not ideal planar surface, one expects the PB solution is applicable in about few water layers from the bilayer surface. In this section, we chose to fit the analytic formula from a distance of 3nm from the center of the bilayer to the center of the water. The results of our fitting is shown in Fig. 5 and Table III.

In Fig. 5, typical concentrations of the positive charges of the bilayer head group represented by the atom  $N^+$ , of the negative mobile counterions  $Br^-$ , and the fitted PB solution are plotted. The PB solution shows an excellent agreement to our simulated counterion profile suggesting this mean-field theory is highly applicable for calculation of electrostatics of our system.

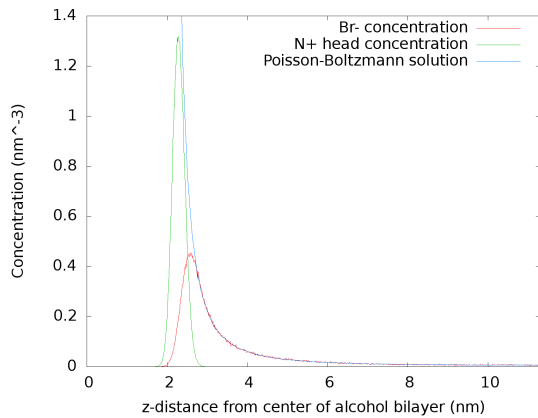


FIG. 5: (Color online) The distribution of the charged atoms in the  $z$ -direction perpendicular to the bilayer for the 100CET system: the  $N^+$  atom concentration of the "upper" leaf (green), the mobile  $Br^-$  counterion concentration (red), and the fitted Poisson-Boltzmann solution (blue) showing excellent agreement in the water layer.

Table III shows the fitting results for various parameters. One sees that the "effective" dielectric constant of our systems is about 75, which is 10% smaller than the known dielectric constant of bulk water in TIP3P model of 82 [24]. Obviously, the presence of the hydrophobic hydrocarbon tail of the bilayer molecules leads to this decrease in the effective dielectric constant as one expects. Knowing  $\Lambda$  and  $\epsilon_w$ , one can calculate the thickness of the water layer  $L_w$  from Eq. (2). This value is listed in column 3 of the Table III. Although,  $L_w$  decreases slightly with increasing cetyl percentage, the total water volume  $V_w = L_x \times L_y \times L_w \approx 1160 \text{ nm}^3$  shown in column 4 is the same for all systems. This is because the same number of water molecules are simulated in all systems. The fitting result shows the consistency of our parameters.

Finally, knowing  $L_w$ , one can calculate the thickness of the bilayer as seen electrostatically by the counterions as  $d = L_z - L_w$ . Column 5 of Table III lists these values for our systems. Clearly as the percentage of shorter cetyl molecules increases, the thickness of the bilayer decreases correspondingly. The total decrease in bilayer thickness from 100% stearyl system to 100% cetyl system is 0.5 nm. Thus, the positively charged cetrimide molecules layers shrink together with the bilayer.

### C. The effect of mixing ratio of cetyl and stearyl alcohol

In this section, the effect of mixing different ratios of cetyl and stearyl alcohol on the physical properties of the bilayer are investigated. As we already mentioned in the previous section, the lateral  $xy$  area of the alcohol is very weakly dependent on the length of the hydrocarbon,

and more on the interaction of the head groups. However, one expects in the  $z$ -component, the length of the hydrocarbon would dictate the thickness of the bilayer as well as regulate the interaction among different bilayers. This is indeed what we observed. Table II shows that as the percentage of the cetyl alcohol molecules increases, the  $z$  dimension of our box decreases monotonically from  $23.38 \pm 0.09$  nm to  $22.68 \pm 0.09$  nm. Since the total amount of water and the pressure are the same for all systems considered, this means the membrane thickness decreases by  $0.155 \pm 0.03$  nm per  $\text{CH}_2$  group (note that the stearyl alcohol bilayer is longer than the cetyl alcohol bilayer by 2 carbon atoms per leaflet, or 4 carbon atoms per bilayer). Accidentally, this is almost the same as the typical length of a C-C bond of 0.154 nm, but that does not mean the hydrocarbon chain is stretched because this length also has to account for the inter-space between the leaflets. Additionally, the shorter hydrocarbon also make the individual molecules tilt more from the  $z$ -axis making the apparent bilayer thickness decreases more.

As it is already known from the experiment data, after a few weeks, the cetyl/stearyl mixture are always more stable than either pure or stearyl alone. It is believed that the reason why the alcohol mixtures is more stable is due to alkyl chain length mismatch [3, 6]. The roughness and irregularities in the leaflets can lead to higher configuration space for the tip of the hydrocarbon tails, as compared to mostly trans configuration for pure alcohol bilayers. Of course, within computer simulation, it is an impossible task to simulate the systems at the length scale of weeks required for stability analysis. Nevertheless, within our micro second time scale, one is already able to elucidate aspects of the molecular picture of the increased configuration space of the tail tips. This is indeed the case from our simulation results.

In order to analyze this configuration entropy of the chain tips, one calculates the deuterium order parameter,  $-s_{CD}$ . This is a sensitive measure of the structural orientation and flexibility of the alcohol molecules in the bilayers (for review, see Ref. [25]). Its definition is given by

$$s_{CD} = \left\langle \frac{3 \cos^2 \theta - 1}{2} \right\rangle \quad (4)$$

where the time dependent  $\theta$  is the angle between the C-D (H atom in our case) bond vector and a reference axis ( $z$ -axis in our case). For ideal perfect crystal phase, the C-H bond lies perpendicular to the  $z$  axis, this order parameter is  $-0.5$ . For very flexible bond, such as at very higher temperature, this bond can adopt all available directions and this order parameter is 0. The value  $-s_{CD}$  varies in the range 0 to 0.5 dependent on the order in the system.

On the table Table. IV, the deuterium order parameter,  $-s_{CD}$  for each methyl group along the hydrocarbon

C-atom	100STE	70STE	50STE	30STE	30CET	50CET	70CET	100CET
2	0.300	0.285	0.278	0.269	0.319	0.310	0.306	0.295
3	0.412	0.399	0.391	0.384	0.419	0.411	0.409	0.403
4	0.448	0.440	0.435	0.430	0.450	0.447	0.445	0.442
5	0.462	0.458	0.455	0.453	0.463	0.461	0.460	0.458
6	0.467	0.465	0.463	0.461	0.467	0.465	0.464	0.462
7	0.470	0.467	0.466	0.465	0.469	0.467	0.467	0.465
8	0.471	0.469	0.468	0.466	0.469	0.468	0.468	0.466
9	0.471	0.470	0.468	0.467	0.470	0.469	0.468	0.466
10	0.471	0.469	0.468	0.466	0.470	0.468	0.467	0.465
11	0.470	0.468	0.467	0.465	0.468	0.466	0.466	0.464
12	0.468	0.466	0.464	0.462	0.465	0.462	0.462	0.459
13	0.463	0.460	0.458	0.454	0.458	0.452	0.453	0.450
14	0.454	0.449	0.447	0.442	0.446	0.439	0.438	0.431
15	0.436	0.427	0.420	0.414	0.418	0.407	0.404	0.392
16	0.414	0.396	0.385	0.371	0.383	0.369	0.363	0.347
17	0.375	0.346	0.331	0.311				
18	0.332	0.296	0.279	0.256				

TABLE IV: Deuterium order parameter for the each methyl group along the cetyl and stearyl alcohol molecules.

tails is listed for the longer stearyl and shorter cetyl alcohols. One can obtain many important conclusions from this table. First of all, in the middle of the chains, all the methyl groups have  $s_{CD} = 0.470$  regardless of the mixing ratio. This is also the highest value of this order parameter among all methyl groups. Therefore, one can conclude that the middle of the hydrocarbon chain remain highly ordered and is unaffected by the length mismatch of the alkyl chains. The role of the middle methyl groups is to maintain the structures of the gel or crystal phase.

The second observation one sees from this table is that the tail of the stearyl becomes more flexible, with decreasing  $s_{CD}$  order as the mixing percentage of cetyl increases. This trend happens for both tips of the chain (near the head group and near the end chain). The behaviour is opposite for the cetyl alcohol molecules. As one increases the mixing ratio of stearyl alcohol, the cetyl molecule becomes more ordered with  $-s_{CD}$  increases. Same as for stearyl alcohol, this trend happens to both tips of the chains. Thus, our molecular analysis of the order parameters supports the argument of stability observed experimentally by confirming an increase in configuration entropy of the tips due to the length mismatch. Our results pointed out further that this effect works on the longer chain only. The shorter chain is squeezed and becomes more ordered upon mixing.

The increased disorder of the longer chain, and increased order of the shorter chain also show up when one calculates the area per molecules for individual species. This can be done by projecting the oxygen atom of the polar head group of each alcohol and perform a voronoi construction to calculate the area per lipid for individual molecules. The results after averaging are listed in

System	Stearyl	Cetyl	Cetrimide
0CET	19.30±0.09	—	19.76±0.31
30CET	19.37±0.11	19.41±0.18	19.80±0.32
50CET	19.41±0.14	19.48±0.14	19.83±0.32
70CET	19.45±0.19	19.50±0.11	19.84±0.32
100CET	—	19.55±0.09	19.88±0.33

TABLE V: Aveaged area per molecule calculated on invidual molecule basis using voronoi construction method.

Table V. One can observe the same disorder for mixed system similar to the deuterium order parameter analysis. For pure alcohol systems, the standard fluctuations in the area per lipid for both cetyl and stearyl molecules are smaller,  $0.09\text{\AA}^2$ . However, in mixed systems, the magnitude of fluctuations increases by 20-100% to the values  $0.11\text{-}0.19\text{\AA}^2$ . This matches with the physical picture that mixed systems causes higher configurational entropy. Additionally, the mean values of the area per lipid increases for the longer stearyl molecule upon mixing, while the mean value for the area per lipid decreases for the shorter cetyl alcohol. This also agree with the more order structure of cetyl alcohol in the bilayer upon mixing with longer alcohol.

Overall, our analysis supports the current experimental point of view that the stability of our mixed ternary system at long time scale is due to an increase in the configurational entropy of the chain tips due to length mismatch. This leads to more flexibility of the bilayer



to relax and fluctuations around equilibrium concentration. At the same time, we show that in the middle of the chain, the shorter alkyl becomes stiffer.

#### IV. CONCLUSION

In this paper, we investigate the structure of cetyl and stearyl alcohol bilayers at different mixing ratios by using atomistic computer simulation. Unlike typical unified atom models, our atomistic model allows one to study additional details in the bilayer such as the deuterium order parameters, area per molecule and fluctuations. The forcefield for our molecules was derived from quantum mechanical calculations and general Amber forcefield for biomolecules.

Structurally, our results agree well with various X-ray experiment data on the system. At the temperature studied of 27°, all our systems exhibit the lamellar phases, specifically the  $\alpha$ -gel and  $L_\beta$  phases, where the local order is hexagonal. The nearest neighbor distance is found to be 4.69Å matches the experimental result. The area per molecule of the cetostearyl alcohol ternary system is numerically found to be 19.5Å<sup>2</sup>, lying within 5% of the experiment value. The electrostatics in the system is well described by the mean-field Poisson-Boltzmann theory with effective dielectric constant reduced compared to bulk water by 10%.

The effect of mixing ratio on the stability of the alcohol ternary system is studied by investigating various

molecular order parameters in our system. The experimental hypothesis for the observed stability of mixed system, as compared to pure alcohol system, is that this is probably due to the increased configurational entropy of individual molecules of the longer alkyl chains. Our analysis of the ordering of molecules in the bilayer supports this hypothesis. The deuterium order parameter for the methyl group at the chain tips for the longer stearyl alcohol decreases upon mixing. Our simulation results provide additional details to this hypothesis, showing that the shorter molecule becomes more ordered upon mixing, leaving more available space to the longer molecule. The in-plane projection for the area per molecule for this species also show stronger fluctuation upon mixing as compared to pure alcohol systems. The shorter molecules is also shown to have difficulty keeping the cetrimide remaining in the bilayer at the simulated molar ratio of various species. It suggests that these system would more stable at lower water and/or cetrimide molar ratio.

Overall, through detail atomistic simulation at one microsecond time scale, we are able to elucidate and quantify several important atomistic details of the mechanism for stability of ternary systems that support current dominant hypothesis as well as the atomistic structure of the bilayer gel.

#### ACKNOWLEDGMENTS

We would like to thank the financial support of the Vietnam National Foundation for Science and Technology NAFOSTED grant number 104.99-2016.39.

- 
- [1] G.M.Eccleston, Colloids and Surfaces A: Physicochemical and Engineering Aspects **123-124**, 169 (1997).
  - [2] H. E. Junginger, Pharmaceutisch Weekblad Scientific Edition **6**, 141 (1984).
  - [3] T. Iwata, Pharm. Tech. Japan **33**, 75 (2017).
  - [4] G.M.Eccleston, International Journal of Pharmaceutics **27**, 311 (1985).
  - [5] G. M. Eccleston, Journal of Pharmacy and Pharmacology **29**, 157 (1977).
  - [6] R. G. Snyder, M. Maroncelli, H. L. Strauss, C. A. Elliger, D. G. Cameron, H. L. Casal, and H. H. Mantsch, Journal of the American Chemical Society **105**, 133 (1983), <https://doi.org/10.1021/ja00339a033>.
  - [7] N. Ferrando, V. Lachet, J.-M. Teuler, and A. Boutin, The Journal of Physical Chemistry B **113**, 5985 (2009), pMID: 19344171, <https://doi.org/10.1021/jp810915z>.
  - [8] J. P. M. Jmbeck and A. P. Lyubartsev, The Journal of Physical Chemistry B **116**, 3164 (2012), pMID: 22352995, <https://doi.org/10.1021/jp212503e>.
  - [9] J. P. M. Jmbeck and A. P. Lyubartsev, Journal of Chemical Theory and Computation **9**, 774 (2013), pMID: 26589070, <https://doi.org/10.1021/ct300777p>.
  - [10] G. Eccleston, M.K. Behan-Martina, G.R.Jones, and E.Towns-Andrews, International Journal of Pharmaceutics **203**, 127 (2000).
  - [11] T. Darden, D. York, and L. Pedersen, J. Chem. Phys. **98**, 10089 (1993), <https://doi.org/10.1063/1.464397>.
  - [12] H. J. Berendsen, D. van der Spoel, and R. van Drunen, Computer physics communications **91**, 43 (1995).
  - [13] M. J. Abraham, T. Murtola, R. Schulz, S. Páll, J. C. Smith, B. Hess, and E. Lindahl, SoftwareX **1**, 19 (2015).
  - [14] W. Humphrey, A. Dalke, and K. Schulten, Journal of Molecular Graphics **14**, 33 (1996).
  - [15] R. Guix-Gonzalez, I. Rodriguez-Espigares, J. M. Ramirez-Angueta, P. Carri-Gaspar, H. Martinez-Seara, T. Giorgino, and J. Selent, Bioinformatics **30**, 1478 (2014).
  - [16] S. Fukushima, M. Takahashi, and M. Yamaguchi, Journal of Colloid and Interface Science **57**, 201 (1976).
  - [17] S. Fukushima, M. Yamaguchi, and F. Harusawa, Journal of Colloid and Interface Science **59**, 159 (1977).
  - [18] I. Langmuir, Proceedings of the National Academy of Sciences of the United States of America **3**, 251 (1917).
  - [19] L. Landau and E. Lifshitz, *Statistical Physics*, Vol. 5 (Elsevier Science, 2013).
  - [20] R. R. Netz, Eur. Phys. J. E **5**, 557 (2001).
  - [21] A. G. Moreira and R. R. Netz, Eur. Phys. J. E **8**, 33 (2002).
  - [22] D. Andelman, in *Handbook of Biological Physics*, Vol. 1, edited by E. S. R. Lipowsky (Elsevier Science B.V., Amsterdam, The Netherlands, 1995) Chap. 12, pp. 603–642.
  - [23] A. Schlaich, E. W. Knapp, and R. R. Netz, Phys. Rev.

- Lett. **117**, 048001 (2016).
- [24] P. G. Kusalik and I. M. Svishchev, Science **265**, 1219 (1994).
- [25] L. S. Vermeer, B. L. de Groot, V. Reat, A. Milon, and J. Czaplicki, Eur. Biophys. J. **36**, 919 (2007).